Available online at www.sciencedirect.com

ScienceDirect

Chinese Journal of Aeronautics 21(2008) 275-280

Chinese Journal of Aeronautics

www.elsevier.com/locate/cja

Liquid–Solid Phase Equilibria of Nb-Si-Ti Ternary Alloys

Bao Jing[a], Huang Qiang[a], Tang Liang[a], Geng Tai[b], Zhao Xinqing[a,*], Ma Chaoli[a]

[a]*School of Materials Science and Engineering, Beijing University of Aeronautics and Astronautics, Beijing 100083, China*

[b]*School of Materials Science and Engineering, University of Science and Technology Beijing, Beijing 100083, China*

Received 5 November 2007; accepted 2 March 2008

Abstract

To determine the liquid–solid phase equilibria of the Nb-Si-Ti ternary system, Nb-Si-Ti alloys of different compositions are prepared. By means of scanning electron microscopy (SEM), X-ray diffraction (XRD) and electron probe microanalysis (EPMA), the phases in the alloys, such as Si-based solutions, Ti(Nb)Si, Ti(Nb)Si_2, Nb(Ti)Si_2, Ti(Nb)$_5Si_4$, Nb(Ti)$_5Si_3$, Ti(Nb)$_5Si_3$, Nb(Ti)$_3$Si and Nb-based solutions are identified, and the phase evolution is analyzed. As a result, the microstructural and microchemical evidence provides a clear definition of the Nb-Si-Ti liquidus surface projection and indicates that the ternary phase diagram has seven transition reactions.

Keywords: Nb-Si-Ti; ternary; phase equilibria; liqudus projection

1 Introduction

As a kind of ultra-high temperature structural materials, niobium-silicide-based in-situ composites have shown full potential for use in advanced gas turbines and aero-engines[1-4]. Nb-Si-Ti-based alloys of multiple alloying components constitute the most promising alloy system because of their ideal combination of high-temperature strength, low-temperature fracture toughness and high-temperature oxidation resistance. Therefore, a thorough understanding of the phase equilibria of ternary Nb-Si-Ti alloys is of utmost importance in elucidating the microstructural phase evolution with the goal of improving the mechanical properties of the alloys[5-10].

There were some reports published with regard to the phase equilibria of the Nb-Si-Ti alloy system based on the experiments or thermodynamic calculation. For example, Bewlay and Jackson investigated the phase equilibria of Nb- and Ti-rich alloys in 1997 and obtained an experimentally estimated liquidus projection of the Nb-Si-Ti system on the Nb- and Ti-rich sides[11]. Liang and Yang presented a liquidus projection of the Nb-Si-Ti system based on thermodynamic calculation successively in 1998 and 2006[12-13]. However, these experimental and calculated results conflict with each other on the scope of some phases as well as at some key points. Earlier experimental investigation on the phase equilibria of the Nb-Si-Ti alloys laid focus on a limited range of compositions.

Nevertheless, to comprehensively understand the phase equilibria of the Nb-Si-Ti system, it is necessary to determine the liquidus projections of the alloys with a broader range of compositions. In this article, an attempt is made to determine the liquid–solid phase equilibria of the Nb-Si-Ti ternary alloys by identifying the specimens with composi-

*Corresponding author. Tel.: +86-10-82338559.
E-mail address: xinqing@buaa.edu.cn
Foundation items: National High-tech Research and Development Program (2006AA03Z102); Aeronautical Science Foundation of China (2006ZF51069)

tions in the full-phase region.

2 Background on Nb-Si-Ti Phase Equilibria

According to the binary phase diagrams of Nb-Si[14-16] and Ti-Si[17-18], in the ternary phase diagram, a eutectic groove should extend between the two binary eutectics. Consequently, there must be a group of liquidus joining $e1_{NbSi}$ and $e1_{TiSi}$, $e2_{NbSi}$ and $e2_{TiSi}$, $e3_{NbSi}$ and $e3_{TiSi}$, respectively (see Fig.1). From the figure, could be observed a ridge from the Nb-37.5Si point at the Nb-Si side to the Ti-37.5Si point at the Ti-Si side, where the intermetallic phases Nb_5Si_3 and Ti_5Si_3 had formed. Between the two eutectic grooves of $e2_{NbSi}$-$e2_{TiSi}$ and $e3_{NbSi}$-$e3_{TiSi}$, a peritectic ridge falls from the peak to both the Si-rich end and the metal-rich end in the phase diagram, and then intersects the liquidus of $e2_{NbSi}$-$e2_{TiSi}$ at U2 and that of $e3_{NbSi}$-$e3_{TiSi}$ at U7. Similarly, a peritectic ridge falls from another peak at a composition of Nb_3Si and Ti_3Si in the opposite directions, and finally intersects the liquidus of $e2_{NbSi}$-$e2_{TiSi}$ at U3 and that of $e3_{NbSi}$-$e3_{TiSi}$ at U1. In addition, the peritectic ridge extends from the binary peritectic falls to the eutectic groove, so there is a peritectic liquidus extending from p_{NbSi} to U6. Similarly, there is a liquidus extending from $p1_{TiSi}$ to U4 and another from $p2_{TiSi}$ to U5.

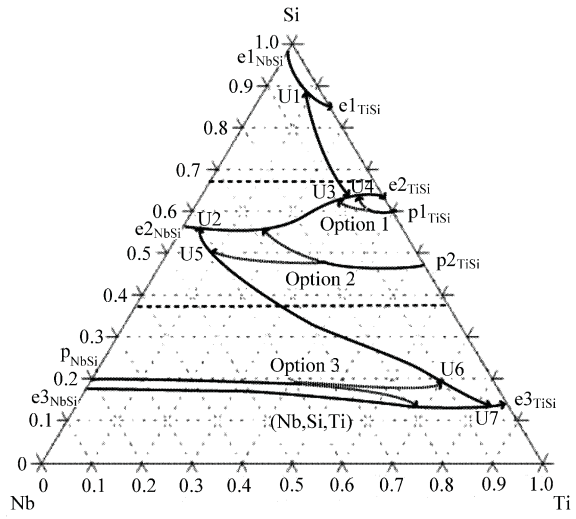

Fig.1 Options for liquidus projection.

However, the ternary phase equilibria are so complicated that the details of the liquidus surface cannot be defined accurately through such a brief analysis. As shown in Fig.1, there are two options for the liquidus of $p1_{TiSi}$: U4 is at the Ti-rich side or at the Nb-rich side of U3. There are also two options for the liquidus of $p2_{TiSi}$: U5 is on the liquidus of $e2_{NbSi}$-$e2_{TiSi}$ or on U2-U7. Similarly, there are two options for the liquidus of p_{NbSi}: U6 is on the liquidus of $e3_{NbSi}$-$e3_{TiSi}$ or on U2-U7. In the following sections, substantiated data will provide the evidence of the correct options for the liquidus. The results and the corresponding reactions are listed in Fig.2, which indicates existence of seven kinds of four-phase equilibrium points. In the article, Nb_5Si_3-containing Ti is referred to as $Nb(Ti)_5Si_3$, and the Ti_5Si_3 with Nb in solid solution is referred to as $Ti(Nb)_5Si_3$. The Nb_3Si with Ti in solid solution is called $(Nb,Ti)_3Si$, because Nb_3Si and Ti_3Si are isomorphous. Similarly, the Nb with Ti and Si in solid solution is known as (Nb,Si,Ti), because there is a continuous bcc solid solution between Nb and Ti at the metal-rich end of the phase diagram at elevated temperatures.

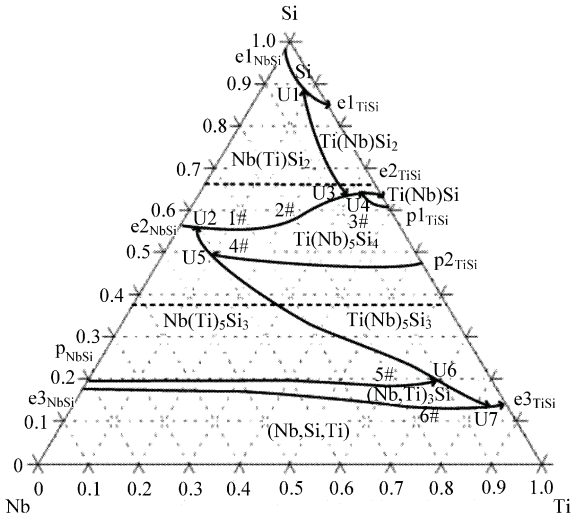

U1: $L+Nb(Ti)Si_2 \rightarrow Si+Ti(Nb)Si_2$

U2: $L+Nb(Ti)_5Si_3 \rightarrow Nb(Ti)Si_2+Ti(Nb)_5Si_4$

U3: $L+Nb(Ti)Si_2 \rightarrow Ti(Nb)Si_2+Ti(Nb)_5Si_4$

U4: $L+Ti(Nb)_5Si_4 \rightarrow Ti(Nb)Si_2+Ti(Nb)Si$

U5: $L+Ti(Nb)_5Si_3 \rightarrow Nb(Ti)_5Si_3+Ti(Nb)_5Si_4$

U6: $L+Nb(Ti)_5Si_3 \rightarrow (Nb,Ti)_3Si+Ti(Nb)_5Si_3$

U7: $L+(Nb,Ti)_3Si \rightarrow Nbss+Ti(Nb)_5Si_3$

Fig.2 Projection of the liquidus surface and the reactions.

3 Experimental

The samples for phase equilibrium investigations were prepared by the non-consumable arc-melting process in an argon atmosphere. The raw material used, contained, 99.9 wt.% Nb, Ti > 99.9% , 99.999 wt.% Si. Alloy ingots were remelted thrice to ensure chemical homogeneity. Table 1 lists the typical compositions of the alloys under investigation and Fig.2 shows the positions representing the chemical compositions. The samples were identified by using an FEI Quanta 600 scanning electron microscopy (SEM) equipped with an energy dispersive X-ray analyzer (IE-350 from Oxford Instruments) working in a back-scattered electron image (BSE) mode. Electron probe microanalysis (EPMA, JXA-8100) was used to determine the chemical composition of the individual phases, and X-ray diffraction (XRD, D/max 2200pc from Regaku) of their crystal structures.

Table 1 Chemical compositions of the Nb-Si-Ti alloys

No.	Alloys	Constituent phases
1#	Nb-56Si-4Ti	PR $Ti(Nb)_5Si_4$; EU $Ti(Nb)_5Si_4$+ $Nb(Ti)Si_2$
2#	Nb-60Si-20Ti	PR $Nb(Ti)Si_2$; EU $Ti_5(Nb)Si_4$ +$Nb(Ti)Si_2$; EU $Ti_5(Nb)Si_4$+$Ti(Nb)Si_2$
3#	Nb-60Si-36Ti	PR $Ti(Nb)_5Si_4$,Ti(Nb)Si; PE Ti(Nb)Si; EU Ti(Nb)Si +$Ti(Nb)Si_2$
4#	Nb-50Si-14Ti	PR $Ti(Nb)_5Si_4$; EU $Ti(Nb)_5Si_4$+$Nb(Ti)Si_2$; EU $Ti(Nb)_5Si_4$+Ti(Nb)Si_2
5#	Nb-21Si-60Ti	PR $Nb(Ti)_5Si_3$, $(Nb,Ti)_3Si$; PE $(Nb,Ti)_3Si$; EU $(Nb,Ti)_3Si$+(Nb,Si,Ti)
6#	Nb-16Si-70Ti	PR $(Nb,Ti)_3Si$; EU $(Nb,Ti)_3Si$+(Nb,Si,Ti); EU (Nb,Si,Ti) +$Ti_5(Nb)Si_3$

PR: primary solidification phase; PE: peritectic solidification phase; EU: eutectic solidification phase

4 Results and Discussion

To illustrate a full picture of liquidus projection of the Nb-Si-Ti alloy system, more than 30 samples with different compositions were prepared. As space was limited, the authors selected only six samples of typical compositions to elucidate the liquid–solid phase equilibria of the Nb-Si-Ti ternary system.

4.1 Nb-56Si-4Ti (1#)

From Fig.3, as the composition of the specimen is close to the four-phase equilibrium point, U2, the microstructure of the as-cast alloy contains two phases, the bright and the dark. The $Ti(Nb)_5Si_4$ phase composed which are the large bright dendrites suggest that it primarily solidifies from the melt having the same composition as that of the phase region, $Ti(Nb)_5Si_4$. The bright network $Ti(Nb)_5Si_4$ and the dark matrix $Nb(Ti)Si_2$ suggest an occurrence of a eutectic reaction of $Ti(Nb)_5Si_4$ + $Nb(Ti)Si_2$.

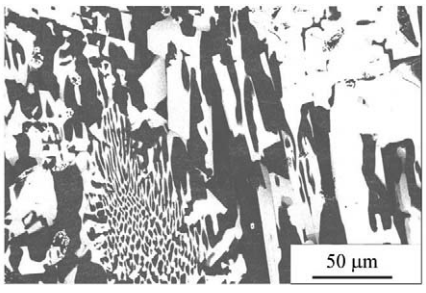

Fig.3 Microstructure of the Nb-56Si-4Ti alloy (1#).

4.2 Nb-60Si-20Ti (2#)

Fig.4 shows the microstructure of the as-cast specimen. The irregular gray dendrites are of the $Nb(Ti)Si_2$ phase primarily grown from the liquid. The bright phase is identified as $Ti(Nb)_5Si_4$. According to the distribution of the $Ti(Nb)_5Si_4$ in the microstructure, the $Ti(Nb)_5Si_4$ phase will probably solidify with $Nb(Ti)Si_2$ in a separated eutectic manner. This is true of the dark phase, $Ti(Nb)Si_2$, which solidifies with $Ti(Nb)_5Si_4$. It is clear that the Nb-60Si-20Ti alloy undergoes two eutectic reactions: $L \rightarrow Nb(Ti)Si_2 + Ti(Nb)_5Si_4$ and $L \rightarrow Ti(Nb)Si_2 + Ti(Nb)_5Si_4$ with a four-phase transition reaction of U3: $L + Nb(Ti)Si_2 \rightarrow Ti(Nb)Si_2 + Ti(Nb)_5Si_4$ between them, which is obviously prohibited because of fast cooling during the preparation of the alloy.

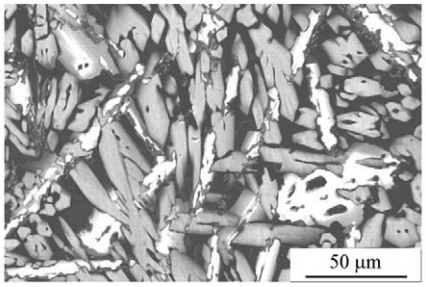

Fig.4 Microstructure of the Nb-60Si-20Ti alloy (2#).

4.3 Nb-60Si-36Ti (3#)

Fig.5 shows the microstructure of the prepared Nb-60Si-36Ti alloy to identify the locus of the peritectic ridge. From the figure, it is noted that the bright primary phase with dendrites in irregular shape is $Ti(Nb)_5Si_4$. Besides, a gray peritectic Ti(Nb)Si phase can be found growing from the primary $Ti(Nb)_5Si_4$, in a peritectic manner. The microstructure also shows a direct growth of primary gray Ti(Nb)Si, in irregular blocks out of the liquid. As a matter of fact, it is observable for eutectic Ti(Nb)Si and dark $Ti(Nb)Si_2$ to grow in an irregular manner.

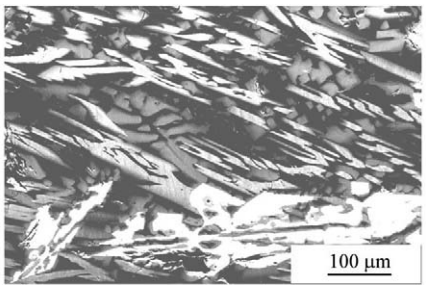

Fig.5 Microstructure of the Nb-60Si-36Ti alloy (3#).

$Ti(Nb)_5Si_4$ is formed from the primary phase, and it is clear that the composition of Nb-60Si-36Ti lies at the single-phase $Ti(Nb)_5Si_4$ region, and the locus of peritectic ridge $p1_{TiSi}$-U4 lies at the Si-rich side of the ternary alloy. As the bright phase has a less volumetric proportion, the composition of Nb-60Si-36Ti comes very close to the peritectic ridge, and the locus of $p1_{TiSi}$-U4 can be defined accordingly.

4.4 Nb-50Si-14Ti (4#)

As shown in Fig.6, the as-cast microstructure of the Nb-50Si-14Ti alloy contains three regions: the gray, the bright and the dark. The bright phase with irregular-shaped dendrites is comprised of the primary phase, $Ti(Nb)_5Si_4$; the gray phase is comprised of $Nb(Ti)Si_2$ and the dark is comprised of $Ti(Nb)Si_2$. Based on the morphology of the phases, the Nb-50Si-14Ti alloy consists of the region of single-phase $Ti(Nb)_5Si_4$. After the primary separation of $Ti(Nb)_5Si_4$, the remaining melt experiences two eutectic reactions of $L \rightarrow Nb(Ti)Si_2 + Ti(Nb)_5Si_4$ and $L \rightarrow Ti(Nb)Si_2 + Ti(Nb)_5Si_4$ in separated eutectic manners.

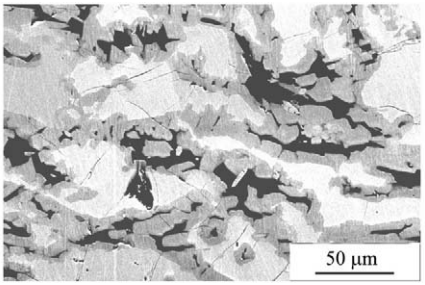

Fig.6 Microstructure of the Nb-50Si-14Ti alloy (4#).

4.5 Nb-21Si-60Ti (5#)

Fig.7 shows the microstructure of the Nb-21Si-60Ti, which helps to identify the locus of the peritectic ridge of U2-U7 and p_{NbSi}-U6. The phase that grows first is the dark primary $Nb(Ti)_5Si_3$. This process lasts for such a short time that it makes up only a few parts of the whole volume. Subsequently, the solidification falls across the peritectic ridge making gray, faceted, and peritectic $(Nb,Ti)_3Si$ grow out of the primary $Nb(Ti)_5Si_3$. From the microstructure, it is noted that the irregularly-shaped gray $(Nb,Ti)_3Si$ has grown directly from the liquid. This leads to an ultimate mixture of bright eutectic (Nb, Si,Ti) and gray eutectic $(Nb,Ti)_3Si$.

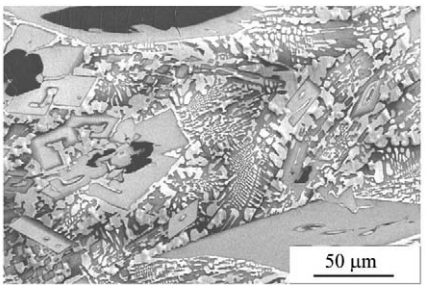

Fig.7 Microstructure of the Nb-21Si-60Ti alloy (5#).

From the formation of primary phase $Nb(Ti)_5Si_3$, it can be identified that the composition of Nb-21Si-60Ti lies in the region of single-phase $Ti(Nb)_5Si_3$. On the other hand, the locus of the peritectic ridge U2-U7 is at the Ti-rich side of the composition Nb-21Si-60Ti, and the peritectic ridge p_{NbSi}-U6 is at the metal-rich side of the composition Nb-21Si- 60Ti.

4.6 Nb-16Si-70Ti (6#)

The microstructure of this alloy is investigated to identify the locus of the peritectic ridge U6-U7 and the eutectic groove $e3_{NbSi}$-$e3_{TiSi}$. As shown in Fig.8, the primary phase is gray, faceted $(Nb,Ti)_3Si$, suggesting that this alloy lies in the $(Nb,Ti)_3Si$ phase region. There are two distinctly eutectic regions: one is bright and gray $(Nb,Ti)_3Si$ and Nbss; the other is bright Nbss and dark $Ti(Nb)_5Si_3$, both are in typical eutectic manners. Between the two eutectic reactions, there is a four transition reaction of U7: $L+ (Nb,Ti)_3Si \rightarrow Nbss + Ti(Nb)_5Si_3$. Note that there are a few black $Ti(Nb)_5Si_3$ in some regions. This is probably ascribed to the composition which is very close to the locus of the peritectic U6-U7 and causes the components to segregate to some extent.

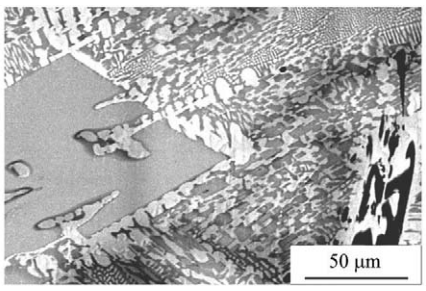

Fig.8 Microstructure of the Nb-16Si-70Ti alloy (6#).

5 Conclusions

The microstructures and the phase equilibria of the ternary Nb-Si-Ti alloys of different compositions are subjected to a systematical investigation, which leads to the following constituent phases: Si, Ti(Nb)Si, $Ti(Nb)Si_2$, $Nb(Ti)Si_2$, $Ti(Nb)_5Si_4$, $Nb(Ti)_5Si_3$, $Ti(Nb)_5Si_3$, $(Nb,Ti)_3Si$, and (Nb,Si,Ti). Through the examination of the phase morphology and phase evolution, a clear definition of the Nb-Si-Ti liquidus surface projection is achieved and the following transition reactions are determined on the basis of microstructural and microchemical evidence:

$$L + Nb(Ti)Si_2 \rightarrow Si + Ti(Nb)Si_2$$
$$L + Nb(Ti)_5Si_3 \rightarrow Nb(Ti)Si_2 + Ti(Nb)_5Si_4$$
$$L + Nb(Ti)Si_2 \rightarrow Ti(Nb)Si_2 + Ti(Nb)_5Si_4$$
$$L + Ti(Nb)_5Si_4 \rightarrow Ti(Nb)Si_2 + Ti(Nb)Si$$
$$L + Ti(Nb)_5Si_3 \rightarrow Nb(Ti)_5Si_3 + Ti(Nb)_5Si_4$$
$$L + Nb(Ti)_5Si_3 \rightarrow (Nb,Ti)_3Si + Ti(Nb)_5Si_3$$
$$L + (Nb,Ti)_3Si \rightarrow Nb + Ti(Nb)_5Si_3$$

References

[1] Subramanian P R, Mendiratta M G, Dimiduk D M. High temperature silicides and refractory alloys. Mat Res Soc Symp Proc 1994; 332: 491-501.

[2] Zhao J C, Westbrook J H. Ultrahigh-temperature materials for jet engines. MRS Bull 2003; 28(9): 622-631.

[3] Subramanian P R, Mendiratta M G, Dimiduk D M. The development of Nb-based advanced intermetallic alloys for structural applications. JOM 1996; 48(1): 33-38.

[4] Jackson M R, Bewlay B P, Rowe R G, et al. High-temperature refractory metal-intermetallic composites. JOM 1996; 48(1): 39-44.

[5] Bewlay B P, Jackson M R, Zhao J C, et al. A review of very-high-temperature Nb-silicide-based composites. Metallurgical and Materials Transactions A 2003; 34(10): 2003-2047.

[6] Subramanian P R, Mendiratta M G, Dimiduk D M, et al. Advanced intermetallic alloys-beyond gamma titanium aluminides. Materials Science and Engineering 1997; 239-240: 1-13.

[7] Mendiratta M G, Dimiduk D M. Deformation and fracture behavior of Nb/Nb_5Si_3 in-situ composites. Metall Trans A 1993; 24: 501-504.

[8] Mendiratta M G, Lewandowski J J, Dimiduk D M. Microstructures and s trength of Nb/Nb_5Si_3 in-situ composites. Metall Trans A 1991; 22: 1573-1583.

[9] Jackson M R, Bewlay B P, Zhao J C, et al. Nb-based silicide composite compositions. US Patent 6428910. 2002: 642-689.

[10] Bewlay B P, Jackson M R, Lipsitt H A. The balance of mechanical and environmental properties of a multielement niobium-niobium silicide-based in situ composite. Metall Mater Trans A 1996; 27: 3801-3808.

[11] Bewlay B P, Jackson M R, Lipsitt H A. The Nb-Ti-Si ternary phase diagram: evaluation of liquid-solid phase equilibria in Nb-

and Ti- rich alloys. J Phase Equilib 1997; 18(3): 264-278.

[12] Liang H, Chang Y A. Thermodynamic modeling of the Nb-Si-Ti ternary system. Intermetallics 1999; 7(5): 561-570.

[13] Yang Y, Bewlay B P, Chang Y A. Liquid-solid phase equilibria in metal-rich Nb-Ti-Hf-Si alloys. J Phase Equilib Diff 2007; 28(1): 107-114.

[14] Knapton A G. The system niobium-silicon and the effect of carbon on the structures of certain silicides. Nature 1955; 175: 730.

[15] Samsonov G V, Neshpor V S, Ermakova V A. Properties of Nb-Si alloys. Neorg Khim 1958(4): 868-878.

[16] Kocherzhinskiy Y A, Yupko L M, Shishkin E A. Equilibrium diagram of the Nb-Si system. Akad Nauk SSSR Met 1980(1): 184-188.

[17] Hansen M, Kessler H D, McPherson D J. Ti-Si phase diagram. Trans ASM 1952; 44: 518-538.

[18] Svechnikov V N, Kocherzhisky Y A, Yupko L M, et al. Phase diagram of the Ti-Si system. Akad Nauk SSSR 1970(2): 393-396.

Biographies:

Bao Jing Born in 1983, she received M.S. from Beijing University of Aeronautics and Astronautics in 2008. She works in Chengdu Aircraft Industrial Co. Ltd now.
E-mail: bj-401@163.com

Zhao Xinqing Born in 1962, he received Ph.D. from the Institute of Metal Research, Chinese Academy of Science in 1995. He is a Professor in Beijing University of Aeronautics and Astronautics now.
E-mail: xinqing@buaa.edu.cn